Plasmoids Formation During Simulations of Coaxial Helicity Injection in the National Spherical Torus Experiment

F. Ebrahimi[1] and R. Raman[2]
[1]Department of Astrophysical Sciences, Princeton University, Princeton, New Jersey 08543, USA
[2]University of Washington, Seattle, Washington 98195, USA
(Received 2 March 2015; published 20 May 2015)

The formation of an elongated Sweet-Parker current sheet and a transition to plasmoid instability has for the first time been predicted by simulations in a large-scale toroidal fusion plasma in the absence of any preexisting instability. Plasmoid instability is demonstrated through resistive MHD simulations of transient coaxial helicity injection experiments in the National Spherical Torus Experiment (NSTX). Consistent with the theory, fundamental characteristics of the plasmoid instability, including fast reconnection rate, have been observed in these realistic simulations. Motivated by the simulations, experimental camera images have been revisited and suggest the existence of reconnecting plasmoids in NSTX. Global, system-size plasmoid formation observed here should also have strong implications for astrophysical reconnection, such as rapid eruptive solar events.

DOI: 10.1103/PhysRevLett.114.205003 PACS numbers: 52.65.Kj, 52.30.Cv, 52.35.Vd, 52.55.Fa

Magnetic reconnection, the rearrangement of magnetic field topology of plasmas, energizes many processes in nature, such as solar and stellar flares, magnetospheres, coronas of accretion disks, and astrophysical jets. Magnetic reconnection has also been demonstrated to be critical in the nonlinear dynamics of many processes in toroidal fusion plasmas, such as sawtooth oscillations, plasma disruption, plasma relaxation, and magnetic self-organization (see, for example, [1]). Sweet-Parker (S-P) steady-state reconnection [2,3] as a local approach and spontaneous magnetic reconnection as the result of tearing fluctuations [4,5] have been the two primary physical models used to explain these processes. Although these models with classical dissipative rates (in which the reconnection rate scales with the Lundquist number with a negative power) have not been able to explain fast reconnection rates in astrophysical systems (with large Lundquist numbers) or the fast time scales of sawtooth crashes, they have explained major reconnection signatures such as strong outflows or growth phase and current and momentum relaxation [6,7]. Sweet-Parker type forced magnetic reconnection in laboratory plasmas [8,9] and spontaneous reconnection (nonaxisymmetric tearing instabilities) in toroidal fusion plasma has been extensively but separately studied. However, the Sweet-Parker type forced reconnection and spontaneous reconnection can be related through plasmoid instability.

In large-scale collisional plasmas with sufficiently high Lundquist numbers, elongated S-P current layers become tearing unstable and break up into multiple islands or plasmoids [10,11]. According to linear theory [12], the instability has a super-Alfvénic growth rate increasing with S as $S^{1/4}V_A/L$ and the number of plasmoids increasing as $S^{3/8}$, where S is the dimensionless Lundquist number $S = LV_A/\eta$, V_A is the Alfvén velocity based on the reconnecting magnetic field, L is the current sheet length, and η is the magnetic diffusivity. In recent years, several authors have developed systematic theoretical and numerical MHD and fully kinetic studies of plasmoid instability in slab geometries (with equilibria such as Harris sheet type models) [13–17]. It has been found that plasmoids allow a fast reconnection rate in the resistive MHD model, nearly independent of the Lundquist number at high S. These recent developments have taken the reconnection model of resistive MHD beyond the S-P model and made the MHD model again relevant for fast reconnection. However, effects beyond MHD may also contribute to fast reconnection as the current sheet width (δ_{sp}) becomes smaller than the two-fluid or kinetic scales [18,19]. Secondary islands (plasmoids) have also been seen in reduced MHD simulations during the nonlinear evolution of the tearing instability in slab geometry [20] and during the nonlinear growth of an internal kink mode in cylindrical geometry [21,22]. In these studies, it was concluded that for realistic fusion relevant parameters, it is the inclusion of two-fluid effects, not the plasmoid instability, that may lead to the fast sawtooth reconnection [22]. Despite the numerous observational evidence of plasmoidlike structures in Earth's magnetosphere and the solar atmosphere [11,23], this instability has not been reported to exist in a laboratory plasma or a fusion device.

In this Letter, we examine the plasmoid formation instability in a large toroidal fusion plasma experiment using resistive MHD simulations. The novel characteristic of these simulations is that they have been performed in a realistic experimental geometry that includes currents driven in the external toroidal and poloidal field coils. It is demonstrated that during transient coaxial helicity injection (CHI) discharges at high Lundquist number,

 © 2015 American Physical Society

the elongated current sheet formed through a Sweet-Parker forced reconnection process breaks up, and transition to a spontaneous reconnection (plasmoid instability) occurs. The transition to plasmoid instability is identified through (1) the breakup of the elongated current sheet, (2) the increasing number of plasmoids with Lundquist number, and (3) the reconnection rate, as it becomes nearly independent of S. Plasmoid formation has importance for the fast flux closure observed during the experiments, because the simulations predict that the reconnection rate in the presence of plasmoids is faster than the S-P reconnection rate. Motivated by these simulations, old experimental camera images have been reexamined. Interestingly, these images from the large NSTX spherical torus (ST) experiment (major radius = 0.86, minor radius = 0.65 m) suggest the existence of reconnecting plasmoids.

In this Letter, the formation of an elongated current sheet and the transition to plasmoid instability is shown to occur in the absence of any preexisting instability, i.e., tearing or kink instability. This transition is examined during transient CHI, a form of electrostatic helicity injection and noninductive current drive. Transient CHI, which is a leading candidate for plasma start-up and current formation in NSTX and NSTX-U, has generated toroidal current on closed flux surfaces without the use of the conventional central solenoid [24]. Elimination of the central solenoid is necessary for a low aspect ratio ST based reactor. In CHI, as shown in Fig. 1, by driving current along the open field lines (the injector current I_{inj}), helicity is injected through the linkage of toroidal flux with the poloidal injector flux. Plasma and open field lines (the magnetic bubble) expand into the vessel if the injector current exceeds a threshold value (for details see [24,25]). Understanding the dynamics and the mechanism of closed flux surface formation during transient CHI is of great importance for the extrapolation of the concept to larger devices and is being studied for the NSTX configuration. In Ref. [26], using a systematic approach using MHD simulations, the fundamental reconnection mechanism that leads to the generation of closed flux surfaces was explained. As also shown through the evolution of poloidal flux surfaces in Figs. 1(b)–1(d), it was found that closed flux surfaces expand in the NSTX global domain through a local S-P type reconnection [26,27]. Motivated by these simulations of forced magnetic reconnection (a universal concept similar to the solar corona's reconnection), it was recognized that the CHI discharges from the large NSTX device may also provide a rich platform for investigating further fundamental reconnection physics, in particular, whether there is a transition to a spontaneous instability.

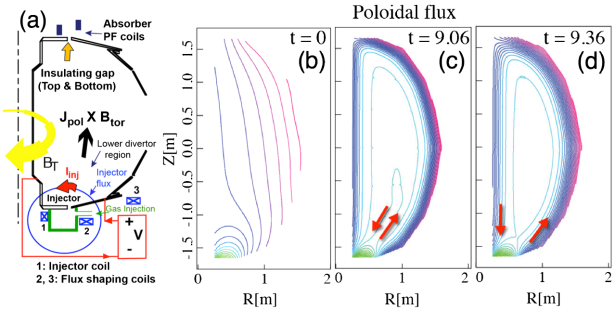

FIG. 1 (color online). (a) Line drawing showing the main components in NSTX required for plasma start-up using CHI. The initial poloidal field, the injector flux (shown by the blue ellipse), connecting the inner and outer divertor plates in the injector region is produced using the lower divertor coils (shown with numbers 1, 2, and 3). In the presence of an external toroidal field (B_T), and after gas injection, voltage (V) is applied to the divertor plates at $t = 6$ ms (as in the simulations) to initiate the discharge [24]. The path of I_{inj} from the voltage source to the outer divertor plate, then through the upper part of the injector flux, and back to the voltage source, is shown by the three red arrows. (b)–(d) Poloidal flux evolution during simulations with one plasmoid. After the discharge fills the vessel (c), the voltage is rapidly reduced to zero at $t = 9$ ms. This induces reconnection in the injector region to form closed flux surfaces (d). The arrows show oppositely directed field lines in the injector region where the S-P current sheet forms (c).

To explore the transition to plasmoid instability, we have performed resistive MHD simulations of transient CHI in the NSTX using the NIMROD code [28]. To elucidate the underlying physics, using the NSTX vessel geometry, resistive MHD simulations for a zero pressure model are performed. In these simulations, we use constant poloidal field coil currents to generate the injector flux (fixed boundary flux simulations) shown in Fig. 1(b). The distance between the injector flux footprints is important for driving an effective magnetic reconnection process and achieving maximum flux closure [26]. Here, to access the plasmoid instability regime, S is increased through decreasing the magnetic diffusivity (η) or by increasing injector voltage using narrow flux footprints. The helicity injection model, boundary condition, and geometry are the same as in the earlier papers [27,29]. A uniform number density of 4×10^{18} m^{-3} for a deuterium plasma is used. Axisymmetric ($n = 0$) simulations with poloidal grid 45×90 sixth to eighth order finite elements are performed in the geometry of the experiment. To obtain S scaling, we used magnetic diffusivitites in the range of 2.5–20 m^2/s. The kinematic viscosities are chosen to give a $Pm = 7.5$ (Prandtl number $= \nu/\eta$) for all values of magnetic diffusivitites used here. A simplified waveform of injector voltage with a constant voltage is applied at 6 ms and turned off at 9 ms. After this time, we observe the reconnection process as the field lines are brought together by a radial force.

It is first confirmed by these simulations that at sufficiently high S (larger than 100), the oppositely directed field lines [shown in Fig. 1(c)] in the injector region have sufficient time to reconnect (before dissipating), leading to the formation of closed flux surfaces [Fig. 1(d)]. The

formation of closed flux surfaces begins via a formation of a S-P current sheet in the injection region. In this case, the current sheet is stable and X point formation near the injection region gives rise to flux surface closure. As S is increased (i.e., L/δ_{sp} is also increased), a transition from a stable current sheet to an MHD unstable one occurs. The current sheet formed in our simulation can extend to about $L = 2.5$–3 m, to the extent of the vertical elongation of the NSTX vessel. In this process, the elongated S-P current sheet becomes unstable to tearing instability and plasmoids, accompanied by multiple X points, are formed spontaneously. Poloidal R-Z cuts of toroidal current densities and the Poincaré plots during magnetic reconnection at 2 times for a plasmoid unstable case at $S = 39000$ are shown in Fig. 2. As the field lines reconnect at $t = 9.044$ ms multiple small-scale islands (plasmoids) are formed around $Z \sim -1.4$ to -1.25 m as it is clearly seen from the Poincaré plot in Fig. 2(c). This is because at this time the elongated current sheet already falls into the plasmoid unstable regime ($L/\delta_{sp} \approx 70$). The process is very dynamical. Interestingly, these small plasmoids are transient and gradually merge as more poloidal flux reconnects. As magnetic reconnection continues and more field lines reconnect, the current sheet also continues to elongate. In this process, as the small transient plasmoids [Fig. 2(c)] merge and form a single island at around $R = 0.6$–0.8 m and $Z = -1.5$ to -1.2, shown in Fig. 2(d), two new larger plasmoids at the upper part of the device are formed ($Z \sim -0.5$ and $Z \sim 0.3$ m). The current sheet as shown in Fig. 2(b) has broken up and three new islands form [Fig. 2(d)]. These larger scale islands that spread along the vertical direction are more persistent. However, even these large islands go through a dynamical process and move around and ultimately they do merge. Figures 2(d)–2(f) show the dynamics of these large scale plasmoids as they merge in time. As seen from these Poincaré plots, three islands [Fig. 2(d)] merge to two islands [Fig. 2(e)], two islands merge to one and form closed flux surfaces [Fig. 2(f)].

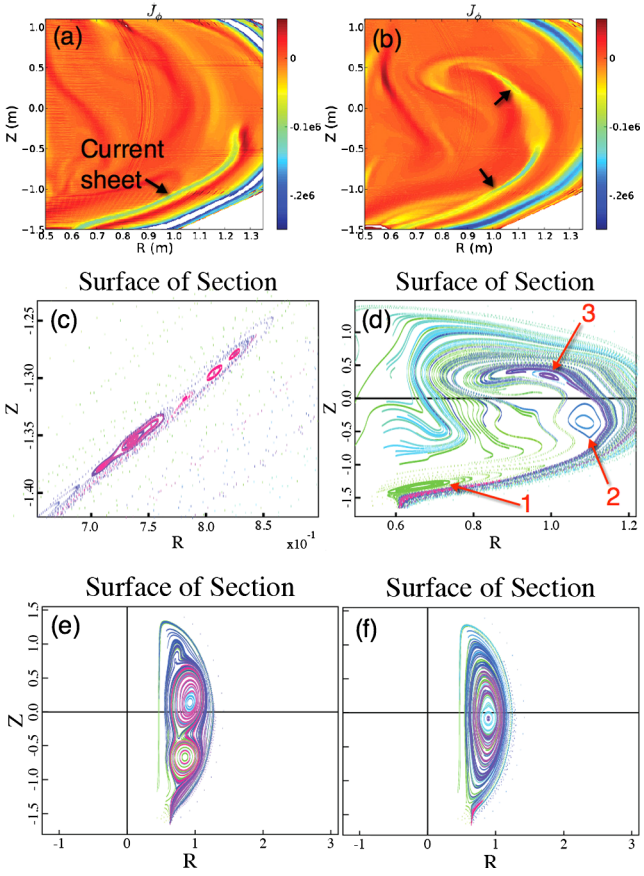

FIG. 2 (color online). (a) and (b) Poloidal R-Z cut of toroidal currents during magnetic reconnection and (c) and (d) Poincaré plots at two times. (a),(c) An unstable elongated current sheet formed (shown in yellow-green $L \approx 1.4$ m) and multiple small scale transient plasmoids formed at the same time ($t = 9.044$ ms). (b) and (d) A large scale breaking of a current sheet to form three larger scale islands is clearly seen, the current sheets between islands is S-P like ($t = 9.174$ ms). (e),(f) Poincaré plots during the evolution of large-scale plasmoids (system-size) into one plasmoid at (e) $t = 9.645$ ms, (f) $t = 10.2$ ms, $S = 39000$. The points in the Poincaré plots are the intersections of a field line with a poloidal plane, as the field line is followed around the torus.

Through Poincaré plots, we have identified the number of plasmoids generated during the magnetic reconnection process. The number of plasmoids generated during magnetic reconnection as S increases are shown in Fig. 3(a). If the current sheet is stable, only a single X point forms (S-P type reconnection) as shown in Fig. 3 for $S < 10^3$.

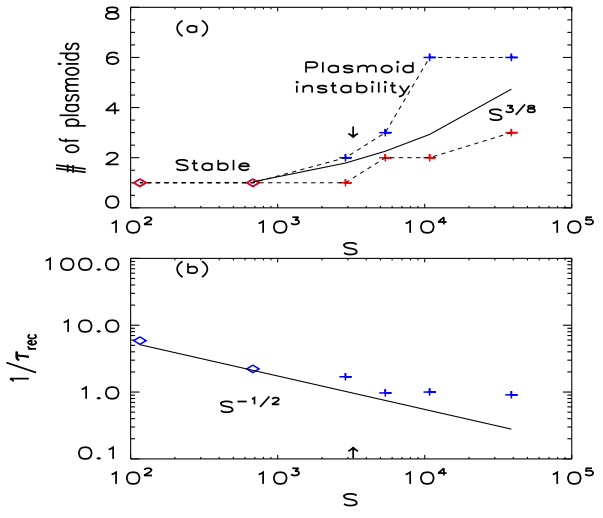

FIG. 3 (color online). (a) Number of plasmoids vs S. Blue: small sized transient plasmoids during the early phase of discharge (Fig. 2). Red: large scale and persistent plasmoids during the later phase of discharge. The solid line is the linear theoretical S scaling. (b) The reconnection rate, $1/\tau_{rec}$ vs S. The transition to plasmoid instability is shown at $S \sim 3000$. The solid line is the S-P scaling.

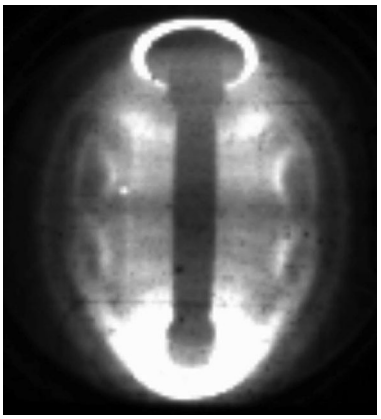

FIG. 4. Camera image during CHI discharge in NSTX shows the formation of two discrete plasma bubble plasmoids.

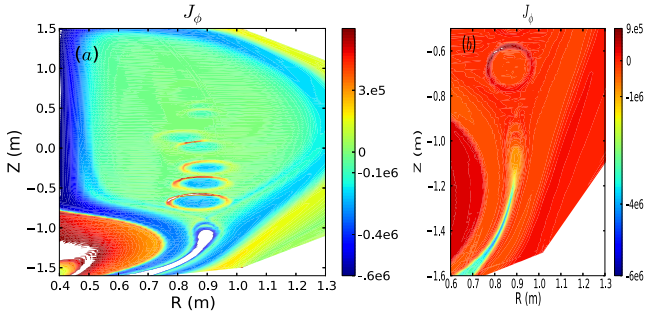

FIG. 5 (color online). Plasmoid formation in MHD simulations of NSTX-U with $\Psi_{inj} = 0.065$ Wb and strong poloidal flux shaping ($t = 7.93$ ms). Poloidal R-Z cut of toroidal currents (a) for the whole device (b) zoom around the injector region.

At approximately $S = 3000$, where the transition to a plasmoid instability occurs, multiple X points form as shown in Fig. 2. The number of small transient plasmoids shown in blue is an increasing function of S. The number of more large scale and persistent plasmoids also increase with S (shown in red). We have also calculated the reconnection time (τ_{rec}) defined here as the time from when the X point is formed until the formation of the largest closed flux volume. Figure 3(b) shows the calculated reconnection rate ($1/\tau_{rec}$) for different values of S as the dynamics goes through a transition to an instability. As it is seen, when the current sheet is stable (S-P type reconnection), the reconnection rate follows the scaling of $S^{-1/2}$ (this regime was studied in [27]). However, as the transition to plasmoid instability occurs, the reconnection rate becomes nearly independent of S, consistent with earlier studies in slab geometries [13,30].

Motivated by the MHD simulations presented here, which show the formation of microplasmoids that tend to merge into a much larger plasma, we have re-examined the very early phase of some NSTX discharges to see if there is any experimental evidence for the formation of these plasmoids. These measurements were carried out using a fast-framing camera that viewed the entire NSTX vessel in a fisheye mode. Although the camera imaging parameters were not optimized for capturing these early, highly dynamic features that are present during the early phase of the discharge, some of the images suggest the formation of plasmoids, an example of which is shown in Fig. 4. The formation and the vertical expansion of toroidally symmetric and plasmoidlike structures are also seen in the movie provided in the Supplemental Material [31]. Although the camera images are encouraging, more detailed measurements are needed in which these images are obtained at higher resolution, and from additional toroidal locations. In addition, measurement of the plasma parameters at the reconnection layer itself are needed to determine the experimental parameter range over which these plasmoidlike features are observed.

To further investigate the formation of plasmoids, we have also performed MHD simulations in the NSTX-U configuration. The location of poloidal flux coils is the same as in the experiment. However, the coils currents in these simulations are optimized to give a very narrow injector flux footprint width [26]. This would give rise to a much more effective forced reconnection compared to NSTX simulations shown above. Because of the much larger reconnecting field ($B = 500$ G), the Lundquist number is as high as 29 000 and well into the unstable regime in NSTX-U. As a result, compared to NSTX cases, plasmoid instability occurs during the injection phase (while the injector voltage is applied). Plasmoid instability with continued injection of plasmoids (up to eight) are observed as shown in Fig. 5(a). The length of the unstable elongated current sheet shown in Fig. 5(b) can reach up to 0.6 m, which is shorter than that obtained above for NSTX.

In summary, in a large-scale toroidal fusion plasma, formation of plasmoids has, for the first time, been demonstrated by simulations, accompanied by promising camera data from experimental observations. Because (i) the high-S plasma regime, which is very difficult to access in experiments designed for reconnection, can be accessed during CHI, and (ii) there is no preexisting plasma or current channel in a transient CHI discharge, the system provides an ideal laboratory for controlling and altering some of the parameters governing S and the current sheet to better understand conditions under which small and large plasmoids are generated. Understanding these plasmoids may be necessary to predict how transient CHI scales as it is extrapolated to future (larger) devices, such as the ST-Fusion Nuclear Science Facility. Plasmoid instability could be the leading mechanism for fast flux closure, and its control may be important for the closed flux plasma stability as considerably larger amounts of poloidal flux are incorporated in future devices to increase the start-up current magnitude. In addition, the two key characteristics of results presented here, (a) fast reconnection, and (b) formation of MHD global system-size plasmoid formation in the presence of a guide field, are relevant to solar

observation of fast reconnecting plasmoids. These results along with future experiments with high-resolution diagnostics could improve our understanding of guide-field reconnection with strong implications for astrophysical plasmas.

Many thanks to Dr. N. Nishino of Hiroshima University for the fast camera measurements. We also acknowledge Dr. H. Ji, Dr. A. Bhattacharjee, Dr. J. Menard, and Dr. S. Prager for useful discussions and comments on this Manuscript. This work was supported by DOE-FG02-12ER55115, DE-FG02-99ER54519, and NSF PHY-0821899 Center for Magnetic Self-Organization. This work was also facilitated by the Max-Planck/Princeton Center for Plasma Physics.

[1] E. G. Zweibel and M. Yamada, Annu. Rev. Astron. Astrophys. **47**, 291 (2009).
[2] P. A. Sweet, in *Electromagnetic Phenomena in Cosmical Physics*, edited by B. Lehnert (Cambridge University Press, Cambridge, England, 1958), Vol. 6 of IAU Symposium, p. 123.
[3] E. N. Parker, J. Geophys. Res. **62**, 509 (1957).
[4] H. P. Furth, J. Killeen, and M. N. Rosenbluth, Phys. Fluids **6**, 459 (1963).
[5] B. Coppi, R. Galvao, R. Pellat, M. Rosenbluth, and P. Rutherford, Sov. J. Plasma Phys. **2**, 19 (1976).
[6] S. Choi, D. Craig, F. Ebrahimi, and S. C. Prager, Phys. Rev. Lett. **96**, 145004 (2006).
[7] F. Ebrahimi, V. V. Mirnov, S. C. Prager, and C. R. Sovinec, Phys. Rev. Lett. **99**, 075003 (2007).
[8] H. Ji, M. Yamada, S. Hsu, and R. Kulsrud, Phys. Rev. Lett. **80**, 3256 (1998).
[9] M. Yamada, H. Ji, S. Hsu, T. Carter, R. Kulsrud, and F. Trintchouk, Phys. Plasmas **7**, 1781 (2000).
[10] D. Biskamp, Phys. Fluids **29**, 1520 (1986).
[11] K. Shibata and S. Tanuma, Earth, Planets, and Space **53**, 473 (2001).
[12] N. F. Loureiro, A. A. Schekochihin, and S. C. Cowley, Phys. Plasmas **14**, 100703 (2007).
[13] A. Bhattacharjee, Y.-M. Huang, H. Yang, and B. Rogers, Phys. Plasmas **16**, 112102 (2009).
[14] R. Samtaney, N. F. Loureiro, D. A. Uzdensky, A. A. Schekochihin, and S. C. Cowley, Phys. Rev. Lett. **103**, 105004 (2009).
[15] Y.-M. Huang and A. Bhattacharjee, Phys. Plasmas **17**, 062104 (2010).
[16] G. Lapenta, Phys. Rev. Lett. **100**, 235001 (2008).
[17] W. Daughton, V. Roytershteyn, B. J. Albright, H. Karimabadi, L. Yin, and K. J. Bowers, Phys. Rev. Lett. **103**, 065004 (2009).
[18] P. A. Cassak, M. A. Shay, and J. F. Drake, Phys. Rev. Lett. **95**, 235002 (2005).
[19] H. Ji and W. Daughton, Phys. Plasmas **18**, 111207 (2011).
[20] N. F. Loureiro, S. C. Cowley, W. D. Dorland, M. G. Haines, and A. A. Schekochihin, Phys. Rev. Lett. **95**, 235003 (2005).
[21] Q. Yu, S. Günter, and K. Lackner, Nucl. Fusion **54**, 072005 (2014).
[22] S. Günter, Q. Yu, K. Lackner, A. Bhattacharjee, and Y.-M. Huang, Plasma Phys. Controlled Fusion **57**, 014017 (2015).
[23] M. Karlický and B. Kliem, Sol. Phys. **266**, 71 (2010).
[24] R. Raman, B. A. Nelson, M. G. Bell, T. R. Jarboe, D. Mueller, T. Bigelow, B. Leblanc, R. Maqueda, J. Menard, M. Ono *et al.*, Phys. Rev. Lett. **97**, 175002 (2006).
[25] T. R. Jarboe, Fusion Technol. **15**, 7 (1989).
[26] F. Ebrahimi, R. Raman, E. B. Hooper, C. R. Sovinec, and A. Bhattacharjee, Phys. Plasmas **21**, 056109 (2014).
[27] F. Ebrahimi, E. B. Hooper, C. R. Sovinec, and R. Raman, Phys. Plasmas **20**, 090702 (2013).
[28] C. R. Sovinec, A. H. Glasser, T. A. Gianakon, D. C. Barnes, R. A. Nebel, S. E. Kruger, D. D. Schnack, S. J. Plimpton, A. Tarditi, M. Chu *et al.*, J. Comput. Phys. **195**, 355 (2004).
[29] E. B. Hooper, C. R. Sovinec, R. Raman, F. Ebrahimi, and J. E. Menard, Phys. Plasmas **20**, 092510 (2013).
[30] N. F. Loureiro, R. Samtaney, A. A. Schekochihin, and D. A. Uzdensky, Phys. Plasmas **19**, 042303 (2012).
[31] See Supplemental Material at http://link.aps.org/supplemental/10.1103/PhysRevLett.114.205003 for a movie version of Fig. 4.